Supporting Information

Molecular Fin Effect from Heterogeneous Self-Assembled Monolayer Enhances Thermal Conductance across Hard-Soft Interfaces

Xingfei Wei[†], Teng Zhang[†], and Tengfei Luo[*,†,‡]

[†]Department of Aerospace and Mechanical Engineering and [‡]Center for Sustainable Energy at Notre Dame, University of Notre Dame, Notre Dame IN 46556, United States

* Corresponding author: tluo@nd.edu

1. Ensemble Average and Convergence of EMD Simulations

For the EMD simulations, we carried out 6 to 11 independent runs, and in each run, we have 4 similar interfaces in the system (Fig. 1 in the main text). The colored curves in Fig. S1a shows the raw thermal conductance data from each of the 44 independent ensembles with respect to the integration time (see Eq. 1 in the main text) for the *hetero-length SAM* interface. The bold black line indicates the ensemble average over all the 44 data sets. For the Green-Kubo correlation method, a single run usually cannot provide converged data due to the lack of ergodicity, especially for slow evolving systems. That is why the curves in Fig. S1a are separated from one another. This is a feature seen also in other Green-Kubo-based quantity evaluations. [1] Using a larger number of ensembles with each starts from a different point in the phase space will help sampling the whole phase space and thus yield the true value of the thermal conductance of the system as indicated by the black curve in Fig. S1a.

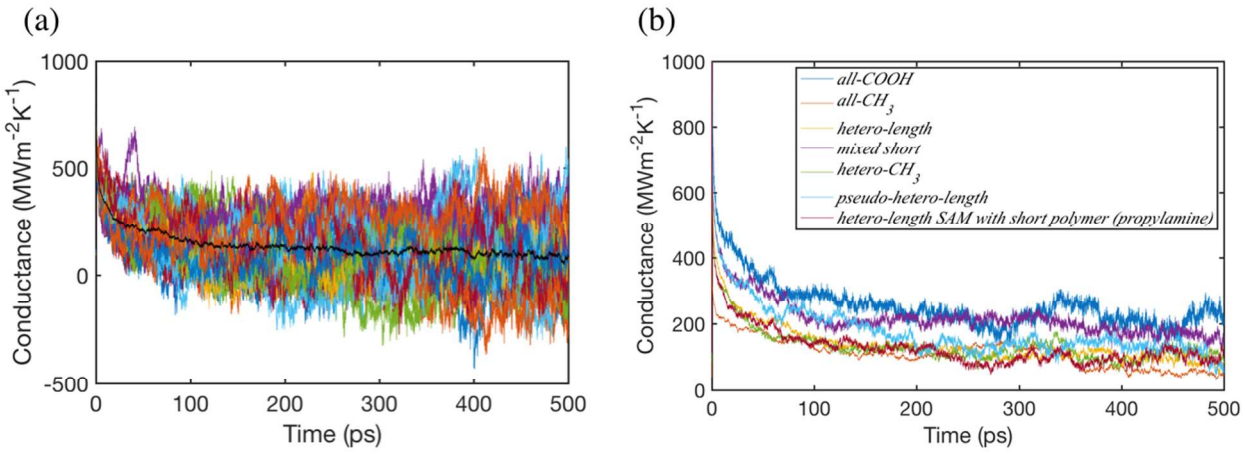

Figure S1. The interfacial thermal conductance calculated by the EMD method with respect to the integration time. (a) Thermal conductance data from independent runs for the *hetero-length SAM* interface and their ensemble average. Each ensemble is represented by a color and the averaged data is shown as the block black curve. (b) Comparison of the ensemble-averaged interfacial thermal conductance for different interfaces. All the liquid side of the interface systems are hexamine, except the last case where a shorter amine, propylamine, is used.

Figure S1b shows all the ensemble averaged EMD results of the interfacial thermal conductance for different interfaces. We can see a good convergence of the ensemble averaged data of the different interfacial thermal conductance values after ~200 ps. We have evaluated three different methods to extract the trend out these curves. In one method, we averaged the thermal conductance over the 400-500 ps period, and those are the data shown in Fig. 3a in the main text. We have also averaged the conductance values from 200 to 500 ps and from 300 to 500 ps, and the compiled data are shown in Fig. S2. All three sets of data show the same trend, which indicates that the results presented in Fig. 3a are robust and reflect the true physics. Moreover, although not in the converged regime, data from 0 to 100 ps in Fig. S1b are most definitively separated from one another and they show the same trend as those presented in Fig. 3a in the main text and Fig. S2. The error bars represent the standard deviation from averaging the data over the given time period.

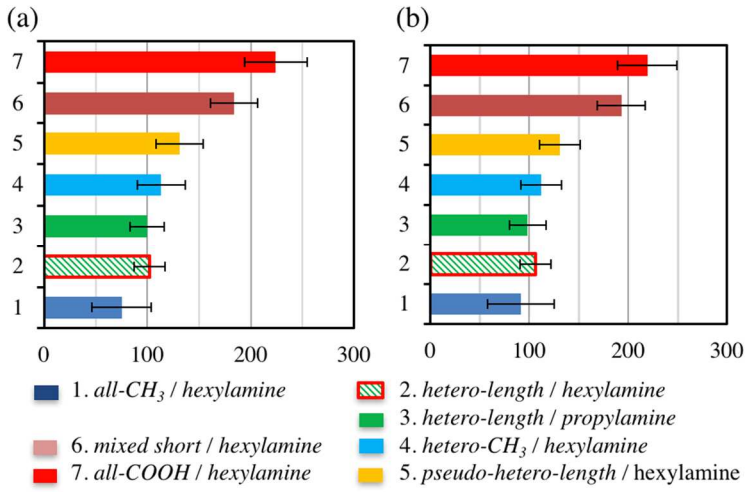

Figure S2. Thermal conductance values obtained from averaging data from (a) 300-500 ps and (b) 200-500 ps.

2. Interfaces with Non-Polar Soft Material – Hexane

Using a non-polar soft material, hexane, can eliminate the effect of H-bonds. Figure S3 shows the EMD results for the interfacial conductance at three different SAM interfaces with hexane as the soft material. Figure S4 shows the averaged conductance values from 200 to 500 ps and from 300 to 500 ps for the hexane systems.

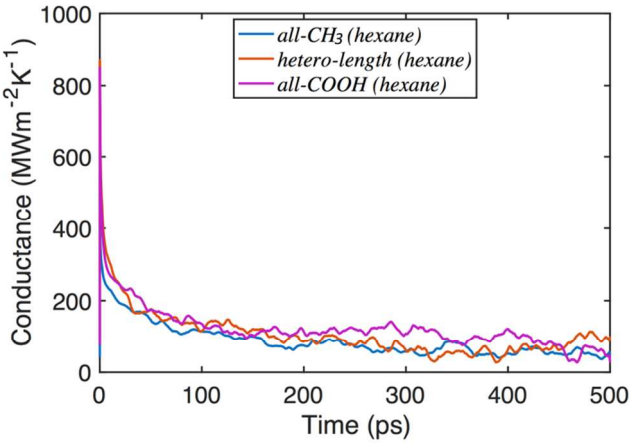

Figure S3. The ensemble averaged interfacial thermal conductance over integration time (see Eq. 2) for three different types of interfaces with non-polar hexane. Using hexane as the soft material, comparison of the averaged interfacial thermal conductance for different types of SAMs from EMD calculation, blue: *all-CH_3 SAM*, orange: *hetero-length SAM*, purple: *all-COOH SAM*.

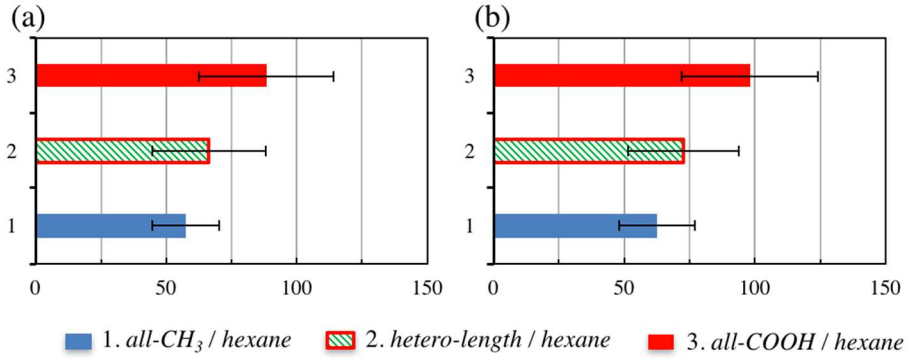

Figure S4. Thermal conductance values obtained from averaging data from (a) 300-500 ps and (b) 200-500 ps for the SAM / hexane interfaces.

3. Force Field Parameters

The parameters used in this study are extracted from BIOVIA Material Studio. [2] The molecular schemes are illustrated in Fig. S5. The atom mass and partial charges are listed in Table S1. The C2 next to the S atom has a partial charge of -0.041 and the C2 next to NA has a partial charge of -0.0233. The pair coefficients between the atoms on the organic molecules are listed in Table S2. The pair coefficients which is associated with the Au is listed in Table S3. The bond, angle, dihedral, and improper styles all use class 2 functionals in LAMMPS, and their parameters are all listed in Tables S4, S5, S6 and S7.

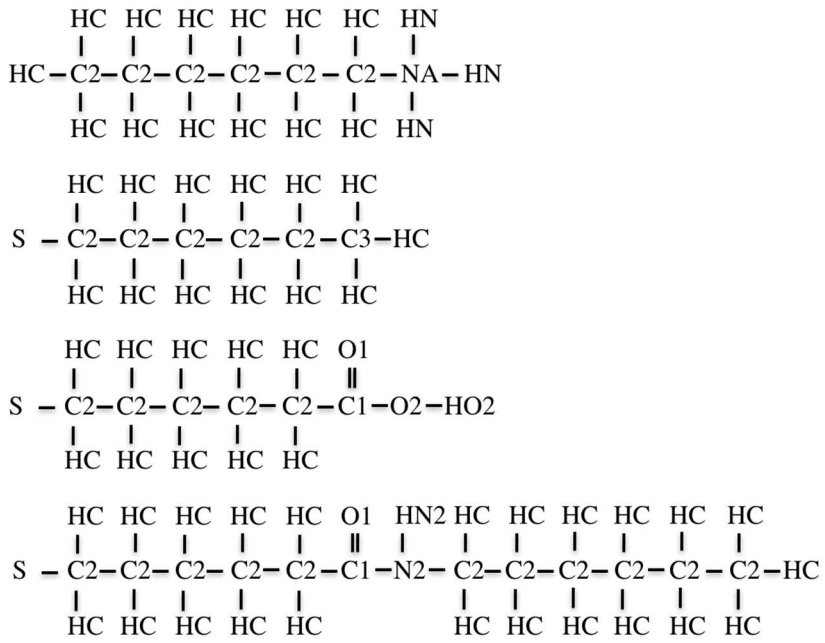

Figure S5. Molecular schemes for (from top to bottom) hexylamine, all-CH_3 SAM, all-COOH SAM, and hetero-length SAM.

Table S1. Atom mass and partial charge.

Atom type	Mass (g/mol)	Charge (e)
C3	12	-0.159
C2	12	-0.106
S	32	-0.065
HC	1	0.053
NA	14	-0.5801
HN	1	0.2487
C1	12	0.702
O2	16	-0.594
O1	16	-0.531
HO2	1	0.423
N2	14	-0.699
HN2	1	0.378
Au	197	0

Table S2. Pair coefficients between particles on the organic molecules.

Pair type	Pair style	ϵ (kcal/mol)	σ (Å)	Cutoff (Å)
C3-C3	lj/class2/coul/cut	0.054	4.010	10
C2-C2	lj/class2/coul/cut	0.054	4.010	10
S-S	lj/class2/coul/cut	0.071	4.027	10
HC-HC	lj/class2/coul/cut	0.020	2.995	10
NA-NA	lj/class2/coul/cut	0.065	4.070	10
HN-HN	lj/class2/coul/cut	0.013	1.098	10
C1-C1	lj/class2/coul/cut	0.120	3.810	10
O2-O2	lj/class2/coul/cut	0.240	3.420	10
O1-O1	lj/class2/coul/cut	0.267	3.300	10
HO2-HO2	lj/class2/coul/cut	0.013	1.110	10
N2-N2	lj/class2/coul/cut	0.106	3.600	10
HN2-HN2	lj/class2/coul/cut	0.013	1.650	10

Table S3. Pair coefficients associated with gold atom.

Pair type	Pair style	D_0 (kcal/mol)	α (1/Å)	r_0 (Å)	Cutoff (Å)
Au-Au	morse	10.954	1.583	3.024	8
Au-S	morse	8.763	1.470	2.650	8

Pair type	Pair style	ϵ (kcal/mol)	σ (Å)	Cutoff (Å)
C3-Au	lj/class2/coul/cut	0.0634	3.182	10
C2-Au	lj/class2/coul/cut	0.0634	3.182	10
HC-Au	lj/class2/coul/cut	0.0414	2.752	10
NA-Au	lj/class2/coul/cut	0.0519	3.097	10
HN-Au	lj/class2/coul/cut	0.0414	2.752	10
C1-Au	lj/class2/coul/cut	0.0634	3.182	10
O2-Au	lj/class2/coul/cut	0.0484	3.026	10
O1-Au	lj/class2/coul/cut	0.0484	3.026	10
HO2-Au	lj/class2/coul/cut	0.0414	2.752	10
N2-Au	lj/class2/coul/cut	0.0519	3.097	10
HN2-Au	lj/class2/coul/cut	0.0414	2.752	10

Table S4. Bond coefficients.

Bond type	r_0 (Å)	K_2 (kcal/mol/Å^2)	K_3 (kcal/mol/Å^3)	K_4 (kcal/mol/Å^4)
C1-C2	1.5202	253.7067	-423.0370	396.9000
C1-O2	1.3683	367.1481	-794.7908	1055.2319
C1-O1	1.2020	851.1403	-1918.4882	2160.7659
C2-C2	1.5300	299.6700	-501.7700	679.8100
C2-HC	1.1010	345.0000	-691.8900	844.6000
C2-S	1.8230	225.2768	-327.7057	488.9722
O2-HO2	0.9520	534.2994	-1287.1937	1889.1396
C1-N2	1.3660	390.6783	-768.3798	923.2418
N2-HN2	0.9959	495.8294	-1092.7239	1441.1290
C2-N2	1.4632	319.1593	-586.3243	961.4143
C2-C3	1.5300	299.6700	-501.7700	679.8100
HC-C3	1.1010	345.0000	-691.8900	844.6000
C2-NA	1.4570	365.8052	-699.6368	998.4842
NA-HN	1.0060	466.7400	-1073.6018	1251.1056

Table S5. Angle coefficients.

Angle type	θ_0 (degree)	K_2 (kcal/mol/radian^2)	K_3 (kcal/mol/radian^3)	K_4 (kcal/mol/radian^4)
C2-C1-O2	100.3182	38.8631	-3.8323	-7.9802
C2-C1-O1	123.1451	55.5431	-17.2123	0.1348
O2-C1-O1	120.7970	95.3446	-32.2869	6.3778
C1-C2-C2	108.5295	51.9747	-9.4851	-10.9985
C1-C2-HC	107.7336	40.6099	-28.8121	0.0000
C2-C2-HC	110.7700	41.4530	-10.6040	5.1290
HC-C2-HC	107.6600	39.6410	-12.9210	-2.4318
C2-C2-C2	112.6700	39.5160	-7.4430	-9.5583
C2-C2-S	112.5642	47.0276	-10.6790	-10.1687
S-C2-HC	107.8522	51.4949	-13.5270	7.0260
C1-O2-HO2	112.8740	53.2512	-14.9979	2.4640
C2-C1-N2	116.9257	39.4193	-10.9945	-8.7733
O1-C1-N2	125.5320	101.8765	-41.8094	0.0000
C1-N2-HN2	122.9480	40.4820	-16.2028	0.0000
C1-N2-C2	122.7520	60.4647	-29.6188	0.0000
C2-N2-HN2	120.1350	29.2218	-14.1448	7.2380
C2-C2-N2	109.8300	76.8966	-48.7334	18.0162
HC-C2-N2	108.5330	66.9202	-13.6480	10.3280
C2-C2-C3	112.6700	39.5160	-7.4430	-9.5583
HC-C2-C3	110.7700	41.4530	-10.6040	5.1290
C2-C3-HC	110.7700	41.4530	-10.6040	5.1290
HC-C3-HC	107.6600	39.6410	-12.9210	-2.4318
C2-C2-NA	111.9100	60.7147	-13.3366	-13.0785
HC-C2-NA	110.6204	51.3137	-6.7198	-2.6003
C2-NA-HN	110.9538	50.8652	-4.4522	-10.0298
HN-NA-HN	107.0671	45.2520	-7.5558	-9.5120

Table S6. Dihedral coefficients.

Dihedral type	K_1 (kcal/mol)	ϕ_1 (degree)	K_2 (kcal/mol)	ϕ_2 (degree)	K_3 (kcal/mol)	ϕ_3 (degree)
O2-C1-C2-C2	1.8341	0.0000	2.0603	0.0000	-0.0195	0.0000
O2-C1-C2-HC	-0.6359	0.0000	1.4807	0.0000	-0.0438	0.0000
O1-C1-C2-C2	0.0442	0.0000	0.0292	0.0000	0.0562	0.0000
O1-C1-C2-HC	-0.1804	0.0000	0.0012	0.0000	-0.0371	0.0000
C2-C1-O2-HO2	-2.5594	0.0000	2.2013	0.0000	0.0325	0.0000
O1-C1-O2-HO2	0.0000	0.0000	2.2089	0.0000	0.0000	0.0000
C1-C2-C2-C2	0.0972	0.0000	0.0722	0.0000	-0.2581	0.0000
C1-C2-C2-HC	-0.0228	0.0000	0.0280	0.0000	-0.1863	0.0000
C2-C2-C2-HC	0.0000	0.0000	0.0316	0.0000	-0.1681	0.0000
HC-C2-C2-HC	-0.1432	0.0000	0.0617	0.0000	-0.1083	0.0000
C2-C2-C2-C2	0.0000	0.0000	0.0514	0.0000	-0.1430	0.0000
C2-C2-C2-S	-0.7017	0.0000	0.0201	0.0000	0.1040	0.0000
S-C2-C2-HC	-0.2078	0.0000	-0.1060	0.0000	-0.3595	0.0000
N2-C1-C2-C2	0.1693	0.0000	-0.0090	0.0000	-0.0687	0.0000
N2-C1-C2-HC	0.1693	0.0000	-0.0090	0.0000	-0.0687	0.0000
C2-C1-N2-HN2	-0.8236	0.0000	2.1467	0.0000	-0.2142	0.0000
C2-C1-N2-C2	-0.7532	0.0000	2.7392	0.0000	0.0907	0.0000
O1-C1-N2-HN2	0.0000	0.0000	2.0521	0.0000	0.0000	0.0000
O1-C1-N2-C2	0.0000	0.0000	2.0521	0.0000	0.0000	0.0000
C2-C2-N2-C1	0.0000	0.0000	0.0000	0.0000	-0.2263	0.0000
HC-C2-N2-C1	0.0000	0.0000	0.0000	0.0000	-0.2263	0.0000
C2-C2-N2-HN2	0.0000	0.0000	0.0000	0.0000	-0.3263	0.0000
HC-C2-N2-HN2	0.0000	0.0000	0.0000	0.0000	-0.3263	0.0000
C2-C2-C2-N2	0.0000	0.0000	0.0000	0.0000	-0.1441	0.0000
HC-C2-C2-N2	0.0000	0.0000	0.0000	0.0000	-0.1441	0.0000
C2-C2-C2-C3	0.0000	0.0000	0.0514	0.0000	-0.1430	0.0000
HC-C2-C2-C3	0.0000	0.0000	0.0316	0.0000	-0.1681	0.0000
C2-C2-C3-HC	0.0000	0.0000	0.0316	0.0000	-0.1681	0.0000
HC-C2-C3-HC	-0.1432	0.0000	0.0617	0.0000	-0.1083	0.0000
C2-C2-C2-NA	0.1764	0.0000	0.1766	0.0000	-0.5206	0.0000
HC-C2-C2-NA	-0.2428	0.0000	0.4065	0.0000	-0.3079	0.0000
C2-C2-NA-HN	-1.1506	0.0000	-0.6344	0.0000	-0.1845	0.0000
HC-C2-NA-HN	-0.5187	0.0000	-0.4837	0.0000	-0.1692	0.0000

Table S7. Improper coefficients.

Improper type	K (kcal/mol/radian^2)	κ_0 (degree)
C2-C1-O2-O1	46.9264	0.0000
C2-C1-O1-N2	24.3329	0.0000
C1-N2-C2-HN2	-5.3119	0.0000

4. Comparison of EMD and NEMD Results

We also used NEMD to calculate the thermal conductance values of three flat SAM interfaces and found reasonable agreement with the values from the EMD calculations (Fig. S6).

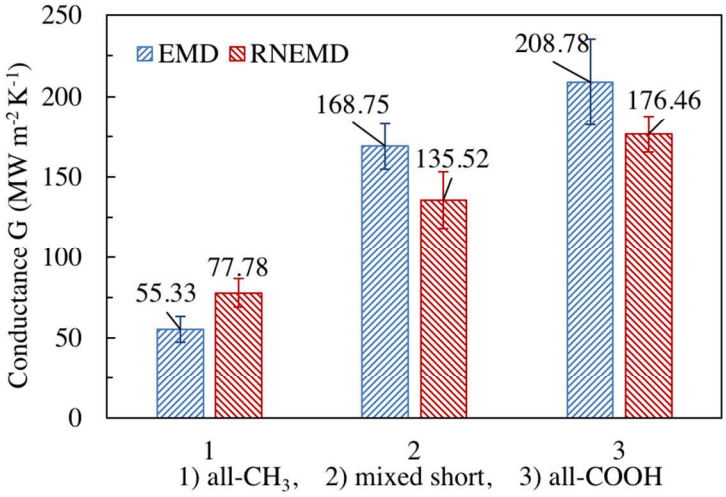

Figure S6. Interfacial thermal conductance values calculated from EMD and NEMD for 1) all-CH_3/hexylamine, 2) mixed short/hexylamine, 3) all-COOH/hexylamine interface systems.

5. Effect of Long Molecular Chain Fraction on Contact Area and Thermal Conductance

Different number of long chain SAM molecules are studied in the *hetero-CH_3 SAM/hexylamine* system. Figure S8 shows that when the fraction of long chain increases from 0% to 16%, the surface area increases by 40% and the thermal conductance increases by 79% (Fig. S7b). When the long chain fraction increases from 16% to 50%, the surface area only increases by 11% and the thermal conductance increases by 11%. Such an observation is interesting. With less long SAM chains (from 50% to 16%), the effective surface area should be smaller. However, the effective contact area (Fig. S7a) does not change much. This can be attributed to that when there are 50% long SAM chains, the space between the long chains are small and liquid penetration is less effective, but when the long chains are more sparse, liquid penetration becomes easier. Despite this observation, the conductance values still scale well with the effective contact area (Fig. S7c), highlighting their inherent correlation.

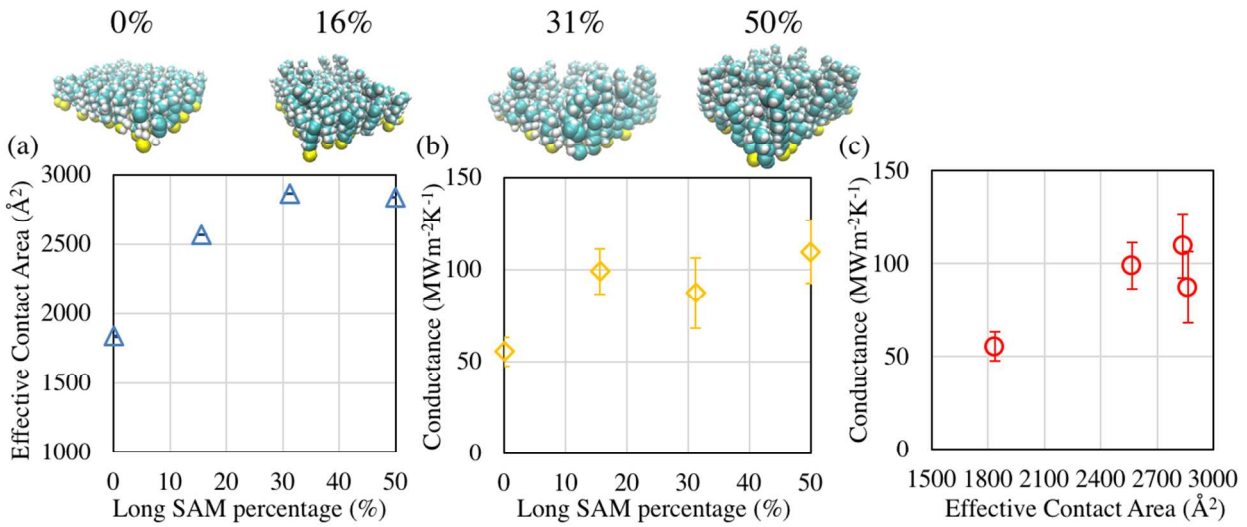

Figure S7. The effect of the fraction of long SAM chain in *hetero-CH_3 SAM/hexylamine* interface on the (a) effective interfacial contact area, (b) interfacial thermal conductance, and (c) interfacial thermal conductance relationship with effective contact area.

6. References

(1). Wang, Z.; Safarkhani, S.; Lin, G.; Ruan, X. Uncertainty quantification of thermal conductivities from equilibrium molecular dynamics simulations. *International Journal of Heat and Mass Transfer* **2017**, 112, 267-278.
(2). *Dassault Systèmes BIOVIA, Materials Studio, Version 8, San Diego: Dassault Systèmes, 2014*.